Original Article

Region-specific proteomic changes in the canine oviduct during oocyte maturation following deslorelin-induced ovulation

Larindhorn Udomthanaisit[1,3] Sittiruk Roytrakul[4] Wirakan Kallayanathum[1,3]
Sudchaya Bhanpattanakul[2,3] Sawanya Charoenlappanit[4] Theerawat Tharasanit[1,3*]

Abstract

Canine reproductive physiology is unique, with oocytes ovulated at an immature stage and completing meiosis within the oviduct. This study investigated protein expression in oviductal secretions from the ampulla and isthmus during oocyte maturation in dogs. Six anestrous female dogs were induced to eestrus using 4.7 mg deslorelin implants, followed by ovariohysterectomy at various time points. Samples were categorized into four groups (n=3 per group) based on oviductal region, histological confirmation, and oocyte maturation status. Proteomic analysis revealed region-specific protein expression changes linked to oocyte maturation. In the ampulla, PRRG4, RCSD1, and UNC13C were downregulated, while CFAP54, ACLY, and MCOLN1 were upregulated, indicating roles in energy metabolism, calcium signaling, and cytoskeletal remodeling. In the isthmus, FCHSD1 and PRKCI were downregulated, while HIC1, ZMYND11, SORCS3, MEGF6, and DYNLRB1 were upregulated, potentially supporting oocyte quality and fertilization competence. These findings highlight dynamic proteomic shifts in the oviductal environment during oocyte maturation in dogs, suggesting the need for further studies to clarify the functional significance of these proteins.

Keywords: canine reproduction, deslorelin, oviductal fluid, oocyte maturation, proteomics

[1]*Department of Obstetrics, Gynaecology and Reproductions, Faculty of Veterinary Science, Chulalongkorn University, Bangkok 10330, Thailand*
[2]*Department of Veterinary Technology, Faculty of Veterinary Technology, Kasetsart University, Bangkok, 10900, Thailand*
[3]*Center of Excellence for Veterinary Clinical Stem Cells and Bioengineering*
[4]*Functional Proteomics Technology Laboratory, National Center for Genetic Engineering and Biotechnology, National Science and Technology Development Agency, Pathum Thani 12120, Thailand*
****Correspondence:*** *Theerawat.T@chula.ac.th* (T. Tharasanit)
Received April 12, 2025
Accepted May 7, 2025
https://doi.org/10.56808/2985-1130.3856

Introduction

Domestic dogs (*Canis familiaris*) exhibit a non-seasonal, monoestrous reproductive cycle, typically undergoing one to two oestrous cycles per year beginning after puberty, which occurs between 6 and 14 months of age (Concannon, 2011). Among mammals, canines possess a particularly distinctive reproductive trait: oocytes are ovulated at the immature germinal vesicle (GV) stage and complete meiosis post-ovulation. Full maturation to the metaphase II (MII) stage occurs within 48-72 hours in the oviduct (Lee and Saadeldin, 2020; Lopes *et al.*, 2007; Tsutsui and Shimizu, 1975). Management of estrous cycle via estrus induction has been extensively studied using various pharmacological agents, including deslorelin, a potent gonadotropin-releasing hormone (GnRH) agonist. Pregnancy rates following deslorelin-induced estrus (63.3%) are comparable to those from natural cycles (66.7%), suggesting that deslorelin does not impair oocyte maturation or reproductive tract function (Walter *et al.*, 2011). A critical determinant of successful oocyte maturation and fertilization is the oviduct, which provides an optimal microenvironment for meiotic resumption. In dogs, oocytes remain in the oviduct for approximately 192-200 hours (Croxatto, 2002), making this extended *in vivo* interaction difficult to replicate *in vitro*. Despite numerous efforts, current *in vitro* maturation (IVM) protocols for canine oocytes remain inefficient, with only 20-30% reaching MII, significantly lower than the more than 80% success rates commonly seen in other species such as cattle and humans (Reynaud *et al.*, 2006). Studies have attempted to optimize IVM through various medium formulations, with or without hormonal or serum supplementation (Apparicio *et al.*, 2011; Astudillo *et al.*, 2023; Lopes *et al.*, 2011; Songsasen *et al.*, 2002), and via co-culture with oviductal cells or oviduct-derived microvesicles (Lange-Consiglio *et al.*, 2017; Lee *et al.*, 2017b; Vannucchi *et al.*, 2006).

A key challenge in improving canine IVM efficiency lies in mimicking the intricate oviductal environment, where the interactions between oocyte and oviductal cells are essential for final maturation (Croxatto, 2002). Recent research has highlighted the role of oviductal exosomes (OC-Exo), which upregulate critical maturation markers in the cumulus oocyte complex (COC), including phosphorylated EGFR and MAPK1/3, GDF9, and BMP15 (Lee *et al.*, 2020). However, studies exploring the molecular landscape of the *in vivo* oviduct remain limited. Prior work has primarily focused on oviduct-specific glycoprotein 1 (OVGP1), which is highly expressed during oocyte maturation and fertilization and appears to be regulated by estrogen (Saint-Dizier *et al.*, 2014).

To address this knowledge gap, the present study investigates protein expression in oviductal secretions from distinct anatomical regions, the ampulla and isthmus, before and after oocyte maturation. By expanding the proteomic understanding of the canine oviductal microenvironment, this research aims to provide deeper insights into canine reproductive biology and inform strategies to enhance *in vitro* fertilization (IVF) and other assisted reproductive technologies (ART) in domestic dogs.

Materials and Methods

Animal and ethical statement: The study was designed as a prospective cross-sectional design. Samples were collected from client-owned dogs presented as clinical cases at the Small Animal Hospital, Faculty of Veterinary Science, Chulalongkorn University, Thailand. The owners provided informed consent before their dogs were enrolled in the study. The experiment received ethical approval in accordance with the guidelines set by the Chulalongkorn University Institutional Animal Care and Use Committee (IACUC), Thailand (Protocol No. 2131027). All procedures were performed in compliance with relevant guidelines and regulations, and adhered to the ARRIVE guidelines. Three biological replicates per group were used, in accordance with previous studies, to capture biological variability, along with three technical replicates to control for technical variation (Ntai *et al.*, 2016).

Six female mixed-breed dogs, aged 3 to 5 years and weighing between 7 and 15 kg, were identified as being in the anestrus stage based on vaginal cytology, which showed fewer than 10% superficial cells, and serum progesterone (P4) levels below 1 ng/mL (Johnston *et al.*, 2001). The dogs were categorized into two groups, including ovulated with immature oocyte and ovulated with mature oocyte according to the criteria specified in Table 1. Following oocyte staging, dogs with mixed stages of oocyte maturation were excluded from the study.

Vaginal cytology examination: Vaginal cells were collected by gently rotating a sterile cotton swab inserted at the vulva's dorsal commissure. The collected cells were transferred to a glass slide, air-dried, and underwent methanol fixation for five minutes, following Leigh *et al.* (2013). The slides were then stained using the Diff-Quick® method for cytological evaluation, as outlined by Johnston *et al.* (2001). Vaginal cytology smears were evaluated by a single trained assessor using a standardized microscopic field method. Approximately 200 to 300 cells per slide were counted at 400× magnification, and the percentage of each cell type was calculated relative to the total number of cells counted. Cell classification followed the methodology described by Reckers *et al.* (2022). Each sample was assessed once, and no multiple independent evaluations were performed.

Progesterone level measurement: Serum progesterone (P4) levels were measured using a radioimmunoassay (RIA) with intra-assay and inter-assay coefficients of variation of 6.27% and 11.63%, respectively. The RIA method was adapted from Kamonpatana *et al.* (1979). Briefly, 0.1 mL of progesterone antibody was added to the serum sample and incubated at room temperature for 1 hour. Tritium-labeled progesterone was then introduced, and the mixture was incubated at 4°C for 18 hours. After incubation, 0.2 mL of activated charcoal was added, and the solution was centrifuged at 1500g for 15 minutes. The supernatant was collected, and the bound radioactivity was measured.

Table 1 The inclusive criteria for sample collection.

Sample group	Vaginal cytology	Progesterone	Oocyte
Ovulated with immature oocyte	Superficial cells > 80%	4-10 ng/mL	Oocyte with confined germinal vesicle
Ovulated with mature oocyte	Superficial cells > 80% with an increase of parabasal cells and intermediate cells	6-15 ng/mL	Oocyte with extrusion of 1st polar body and metaphase II plate

* Modified from the previous studies (Gloria *et al*., 2018; Kutzler *et al*., 2003; Lee *et al*., 2017a; Reckers *et al*., 2022; Saint-Dizier *et al*., 2014)

Estrus induction: Estrus was induced by the subcutaneous implantation of 4.7 mg deslorelin (Suprelorin®, Virbac, New Zealand) into the right shoulder area modified from (Ponglowhapan *et al*., 2018). The implantation date was designated as day 0. Vaginal smears were collected every 48 hours and examined using Diff-Quick® staining, while progesterone (P4) concentrations were measured via RIA.

Collection of canine oviductal secretion: The reproductive organs were examined for the presence of follicles, corpus hemorrhagicum, and corpus luteum. The oviduct was then dissected and divided into two sections, including the ampulla and the isthmus, based on specific anatomical criteria. The ampulla is the longest and widest portion, constituting more than half of the oviduct's total length, and extends craniomedially within the ovarian bursa. The isthmus, the final section of the oviduct, is the thickest, most curved, and shortest part (Evans and De Lahunta, 2012; Kumar, 2015). The isolated ampulla and isthmus were trimmed at both ends and flushed with 100 µL of sterile phosphate-buffered saline (PBS) to collect oviductal secretions from the middle region. The collected secretion was stored at -80°C until proteomic analysis. Anatomical validation of the oviduct tissue was performed using histological examination. In brief, formalin-fixed samples were embedded in paraffin and sectioned at a thickness of 4 µm. The oviducts were stained with hematoxylin and eosin (H&E), and the histological characterization of each oviduct region was performed according to the criteria established by Eurell and Frappier (2013)

Oocyte staining and assessment of the oocyte maturation stage: *In vivo* derived cumulus-oocyte complexes (COCs) were retrieved from the flushed oviductal secretions and processed for further analysis. To minimize the risk of misclassification, direct immunofluorescent staining of oocytes was performed to enable definitive classification of oocyte maturation stages. Following collection, the oocytes were denuded of cumulus cells and examined under a light microscope to assess morphological integrity. The denuded oocytes were then incubated for 45 minutes in a microtubule-stabilizing solution containing glycerol. The stabilization solution was composed of 25% glycerol, 50 mM KCl, 0.5 mM MgCl2, 0.1 mM EDTA, 0.1 mM EGTA, 1 mM 2-mercaptoethanol, 50 mM imidazole, and 4% Triton X-100, as outlined in the protocol by Simerly and Schatten (1993) (Simerly and Schatten, 1993). After incubation, the oocytes were briefly rinsed with PBS supplemented with BSA, fixed in 4% (w/v) paraformaldehyde, and stored for subsequent immunofluorescent staining.

The fixed oocytes were incubated for 1 hour with monoclonal anti-α-tubulin antibody (T5168, 1:100, Sigma, Germany) in PBS containing 0.1% (w/v) bovine serum albumin (BSA) (A3311, Sigma, Germany) and 0.1% (v/v) Triton X-100 (CAS 9002-93-1, Sigma, Germany). The oocytes were subsequently stained with a goat anti-mouse secondary antibody conjugated to tetramethylrhodamine isothiocyanate (TRITC) (T5393, 1:100, Sigma, Germany) in 0.1% BSA/PBS. After two washes in 0.1% BSA in PBS, the oocytes were incubated with Alexa Fluor 488 phalloidin (Molecular Probes, Invitrogen, USA) at a 1:50 dilution in 0.1% BSA/PBS to stain actin microfilaments. Chromatin was labeled with 4′,6-diamidino-2-phenylindole (DAPI) (S33025, Invitrogen, USA) (Thiangthientham *et al*., 2023). Immature oocytes display a diffuse microtubule network without the formation of a meiotic spindle, and the chromatin remains compacted within the ooplasm. In contrast, mature oocytes exhibit a distinct barrel-shaped meiotic spindle at the metaphase plate, with the chromatin centrally aligned and the polar body located in the perivitelline space. The entire process of sample collection is summarized in Figure 1.

Proteomic analysis: The total protein concentration in each secretion sample was determined using the Lowry method, with BSA as the protein standard. Prior to analysis, the proteins were reduced by incubating the samples with 10 mM dithiothreitol (DTT) in 10 mM ammonium bicarbonate for one hour at room temperature. Subsequently, to alkylate the cysteine residues, the samples were treated with 100 mM iodoacetamide (IAA) in 10 mM ammonium bicarbonate in the dark at room temperature for one hour. Proteins were then digested overnight with sequencing-grade trypsin (Promega, Germany) at a 1:20 (w/w) ratio, with the reaction terminated by adding 0.1% formic acid (FA). The resulting tryptic peptides were prepared for analysis using an Ultimate 3000 Nano/Capillary LC System (Thermo Scientific, UK), coupled to a Hybrid quadrupole Q-Tof impact II™ mass spectrometer (Bruker Daltonics), equipped with a Nano-captive spray ion source. A 1 µL volume of the digested peptides was concentrated on a µ-precolumn (300 µm i.d. × 5 mm) C18 PepMap 100, 5 µm, 100 A (Thermo Scientific, UK), and separated on a 75 µm i.d. × 15 cm analytical column packed with Acclaim PepMap RSLC C18, 3 µm, 100Å, nanoViper (Thermo Scientific, UK). The C18 column was maintained in a thermostatic oven at 40°C. The mobile phases included solvent A (0.1% formic acid in water) and solvent B (0.1% formic acid in 80% acetonitrile). Peptides were eluted with a gradient from 5% to 55% solvent B over 30 minutes at a flow rate of 0.30 µL/min. Electrospray ionisation was performed at 1.6 kV using CaptiveSpray, with nitrogen as the drying gas (flow rate: 50 L/h). Collision-induced dissociation (CID)

product ion spectra were generated using nitrogen as the collision gas. Mass spectra (MS) and MS/MS spectra were acquired in positive ion mode at 2 Hz across an m/z range of 150–2200. The collision energy was adjusted to 10 eV according to the m/z value. Each sample was analysed in triplicate using liquid chromatography-mass spectrometry (LC-MS). The MS/MS raw data and analyses have been deposited in the ProteomeXchange Consortium (http://proteomecentral.proteomexchange.org) via the jPOST partner repository (https://jpostdb.org) with the data set identifier JPST003743 and PXD062813 (https://repository.jpostdb.org/preview/6380969756 7f9c1faf1548, accessed key 5980).

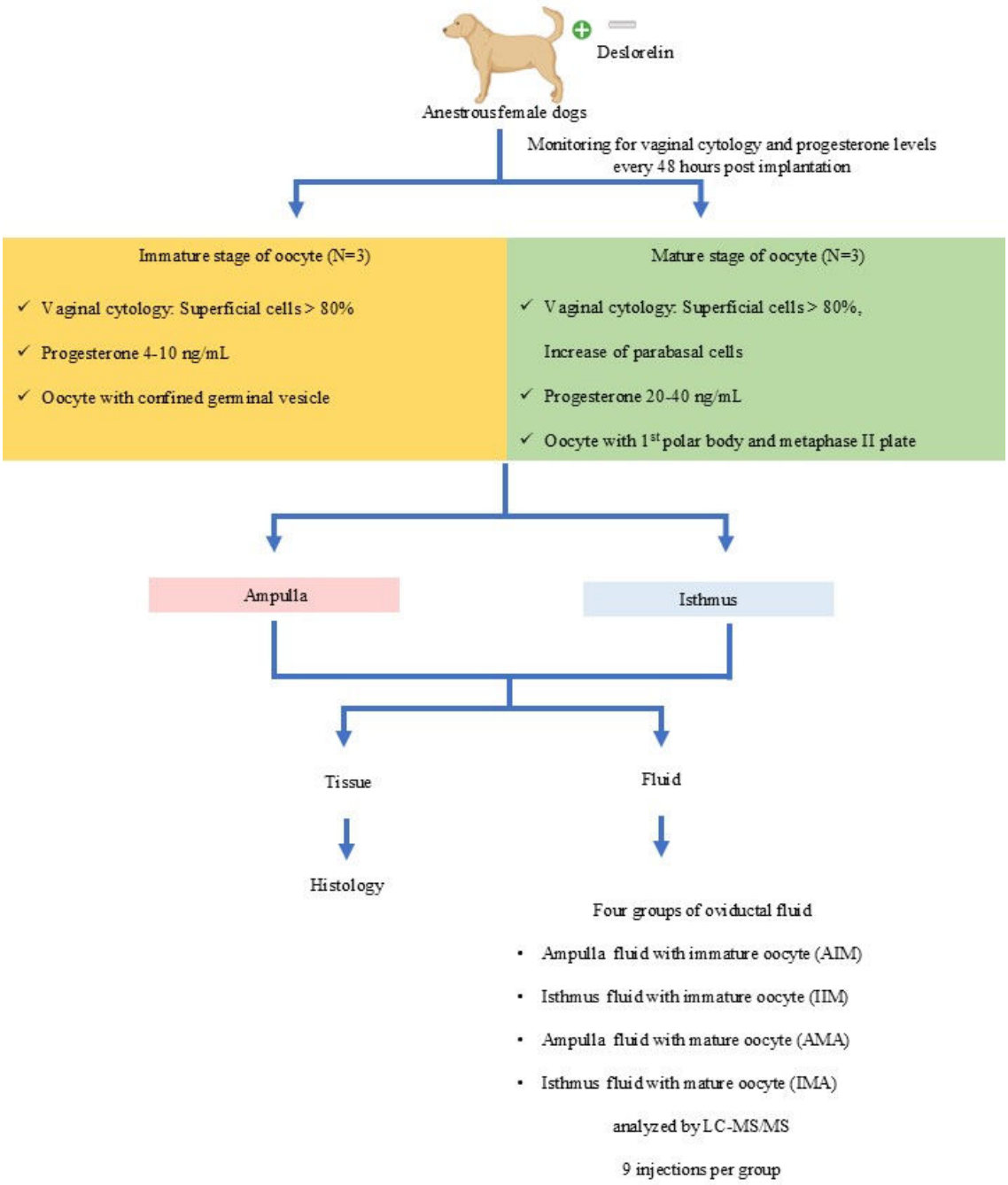

Figure 1 Experimental design of canine oviductal fluid collection. Dogs meeting the criteria following deslorelin implantation underwent ovariohysterectomy for the retrieval of reproductive organs. Refer to the Materials and Methods section for additional details.

Table 2 The descriptive data of individual dogs after Deslorelin implantation.

Sample No.	Implant to proestrus (day)	Implant to OVH* (day)	Progesterone level (ng/mL)	The percentage of vaginal cytology at OVH day				No. of CL**	No. of oocyte (%)	Oocyte stage
				Parabasal Cell	Intermediate Cell	Superficial Cells	Anuclear superficial Cell			
No.1	7	14	12.52	0	0	22	78	15	4 (26.7%)	immature
No.2	6	15	4.59	0	0	16	84	8	6 (75.0%)	immature
No.3	8	14	5.55	5	0	25	70	7	6 (85.7%)	immature
No.4	10	21	5.92	0	1	37	52	5	1 (20.0%)	mature
No.5	8	19	12.3	2	8	18	72	6	2 (33.3%)	mature
No.6	9	17	10	10	11	44	35	10	3 (30.0%)	mature

*OVH: ovariohysterectomy, **CL: Corpus luteum

Bioinformatics and data analysis: Data from liquid chromatography-tandem mass spectrometry (LC-MS/MS) were analysed with MaxQuant software (version 2.2.0.0) (Tyanova *et al.*, 2016) and matched against the Uniprot *Canis lupus familiaris* database for protein identification. Peptide intensities obtained from the LC-MS analysis were log2-transformed. Data normalisation and visualisation of protein abundance changes across groups were carried out using MetaboAnalyst software version 6.0. A volcano plot was applied to analyze statistically significant differences ($p < 0.05$) and fold changes (≥ 2.0 or ≤ 0.5) within each anatomical region by comparing between oocyte maturation stages. To focus on proteins exhibiting the most pronounced and confident differential expression between groups, the top 10 upregulated and top 10 downregulated proteins were selected, highlighting those with statistical significance. Additionally, protein–protein interaction analysis was performed via the STITCH database version 5.0 for data validation.

Result

All six dogs exhibited the first signs of estrus within 10 days post-implantation, achieving a 100% estrus rate in 6–10 days (8 ± 1.41). Ovulation was confirmed in all animals (100% success rate) based on the presence of corpora lutea and occurred between 13 and 21 days post-implantation, as determined by vaginal cytology and serum progesterone (P4) levels (Table 2). P4 concentrations were measured using RIA, with intra- and inter-assay coefficients of variation of 6.27% and 11.63%, respectively. During ovulation with immature oocytes, P4 levels ranged from 4.59 to 12.52 ng/mL (mean: 7.55 ± 4.3 ng/mL), whereas in the group with mature oocytes, levels ranged from 5.92 to 12.3 ng/mL (mean: 9.4 ± 3.2 ng/mL). Vaginal cytology, oviduct histology, and the morphology of mature oocytes are described and illustrated in Figure 2.

For proteomic analysis, individual ampulla secretions were subjected to in-gel digestion followed by LC-MS/MS. A total of 16,377 proteins were identified in the secretion. A heatmap was generated to visualize protein expression profiles between the immature and mature oocyte groups, focusing on the ampulla and isthmus regions. Each row represents a protein, while each column corresponds to an individual sample; red indicates high protein abundance, and blue indicates low abundance. Hierarchical clustering revealed distinct expression patterns between groups, indicating group-specific proteomic signatures. Regions of high abundance highlight proteins potentially more active in one group, whereas regions of low abundance suggest downregulation (Figure 3).

The partial Least Squares Discriminant Analysis (PLS-DA) scores plot in Figure 4 illustrates the separation of four groups based on two principal components. The x-axis (Component 1) accounts for 12.6% of the variation, while the y-axis (Component 2) explains 5.3% of the variation. The four groups shown include ampulla fluid with immature oocyte (AIM, red), Isthmus fluid with immature oocyte (IIM, green), Ampulla fluid with mature oocyte (AMA, dark blue), and Isthmus fluid with mature oocyte (IMA, light blue). Each protein point is enclosed within an ellipse that indicates consistent and distinct proteomic profiles, supported by a 95% confidence ellipses region for that group. The clustering indicates clear separation between groups, with ampulla secretion with mature oocyte and isthmus secretion with immature oocyte distinctly positioned away from ampulla and isthmus fluid of immature stage oocyte. This separation suggests significant differences in protein expression or other variables analyzed, based on both anatomical regions (ampulla vs. isthmus) and maturity stages (immature vs. mature).

The comparison of protein expression between oocyte maturity stages in each anatomical region is presented using a volcano plot with a fold change (FC) threshold of ≥ 2.0 or ≤ 0.5 and a p-value of 0.05. The boxplot of each protein in the ampullar and isthmus was shown in Figures 5 and 6, respectively. Additionally, the top 10 upregulated and downregulated proteins are listed in Table 3.

To investigate the interactions among upregulated and downregulated proteins and key regulators of the reproductive cycle, namely estrogen, progesterone, and the MAPK pathway. The STITCH database (version 5.0) was used. Due to limited data availability for *Canis lupus familiaris*, the *Homo sapiens* database was

selected as an alternative. The resulting protein interaction network is shown in Figure 7. This analysis identified 16 of the top 20 differentially expressed proteins. Among them, PSMC5, ACLY, UNC13C, and MCOLN1 exhibited strong interactions with proteins and hormones involved in the estrous cycle, indicated by thick edges representing high-confidence interaction scores (>0.9). ACLY emerged as a central hub, interacting with key metabolites such as coenzyme A, MgADP, oxaloacetate, and phosphate. HIC1 was also found to interact with estrogen and its receptor. Notably, UNC13C and MCOLN1 were implicated in calcium-mediated signaling due to their strong associations with calcium ions. Other proteins in the network did not show direct connections with known oocyte maturation molecules, suggesting their roles in this biological process may not yet be well characterized.

Discussion

This study explores the proteomic profile of oviductal secretions in dogs, focusing on region-specific protein changes related to oocyte development. The limitation of the study was that all dogs were client-owned and presented as clinical cases, which limited the ability to fully standardize environmental conditions or housing. The potential impact of such confounding factors was acknowledged during data interpretation, and the findings are considered preliminary, requiring further validation under controlled experimental conditions. Estrus was successfully induced in all subjects using deslorelin implants, with a 100% induction rate, which is consistent with previous studies (Borges *et al.*, 2015; Fontaine *et al.*, 2011; Walter *et al.*, 2011). To support the conclusion that deslorelin treatment does not significantly impair reproductive function, a previous study reported that the pregnancy rate following deslorelin-induced estrus (63.3%) was comparable to that observed during natural estrus (66.7%), with no significant difference between the group (Walter *et al.*, 2011). Following ovulation, serum progesterone (P4) concentrations were 7.55 ± 4.3 ng/mL in the group with immature oocytes and 9.4 ± 3.2 ng/mL in the group with mature oocytes. The overlap between these P4 ranges underscores that serum progesterone levels are not directly correlated with oocyte nuclear maturity. Consequently, direct immunofluorescent staining for chromatin configuration and meiotic spindle morphology was employed to accurately determine oocyte maturation stages. This cellular validation approach minimized the risk of sample misclassification due to hormonal overlap and strengthened the reliability of subsequent proteomic analyses. Notably, previous studies have also reported a higher percentage of mature oocytes when serum progesterone concentrations ranged between 6 and 15 ng/mL (Lee *et al.*, 2017b), supporting the relevance of the observed hormonal profiles in the current study.

Although canine oocyte maturation, particularly within the oviduct, is not well understood, this study offers valuable insights. It identified several proteins in the ampullary and isthmic secretions of estrous female dogs, with 20 candidate proteins showing significant upregulation or downregulation, helping bridge the knowledge gap despite challenges in obtaining large sample sizes.

In the ampullary secretions, the downregulation of proteins such as PRRG4, RCSD1, SOWAHD, SFMBT2, and UNC13C during oocyte maturation suggests a functional shift in the reproductive microenvironment from an immature to a mature state. For instance, PRRG4, linked to mitochondrial DNA (mtDNA) content, showed reduced expression as oocytes transitioned to the mature stage, aligning with studies showing a decline in mtDNA as oocytes mature (Mahrous *et al.*, 2012; Wang *et al.*, 2023). Similarly, RCSD1, an actin-organizing protein, exhibited higher expression during the immature stage, suggesting it may contribute to actin remodeling during meiosis resumption. UNC13C, involved in calcium and calmodulin signaling, was more highly expressed during the immature phase, indicating its role in calcium-mediated pathways necessary for meiotic progression and egg activation (Su and Eppig, 2002). These proteins likely support early developmental processes that become less critical once the oocyte matures.

Conversely, proteins such as CFAP54, MCOLN1, ACLY, CXHXorf38, and MYOF were upregulated in the ampullary secretions as oocytes matured. CFAP54, associated with microtubule dynamics in cilia and flagella, may aid in the transport of oocytes or fluids within the oviduct, facilitating a dynamic environment for gamete and embryo movement. ACLY, a marker of oocyte maturation in porcine models (He *et al.*, 2023), was upregulated, reflecting the increased energy demands during oocyte maturation and early embryonic development (Sturmey *et al.*, 2009). MCOLN1, involved in calcium signaling and lysosomal function, is known to regulate calcium homeostasis, and its upregulation suggests a role in calcium-mediated signaling during oocyte maturation (Wakai *et al.*, 2012). These findings indicate a coordinated network of processes in the ampulla, including ciliary function, metabolic support, and enhanced fertilization capability, all of which facilitate successful oocyte maturation.

In the isthmic secretions, downregulation of FCHSD1, LOC119868814 (an uncharacterized protein), PRKCI, and ATP10B during oocyte maturation was observed. FCHSD1 regulates actin polymerization and membrane dynamics (Cao *et al.*, 2013), and PRKCI, a member of the protein kinase C subfamily, contributes to cell polarization and motility (Xiao and Liu, 2013). Their higher expression in the immature stage suggests a role in preparing oocytes for meiotic resumption and spindle assembly. As oocytes mature, these proteins may no longer be needed, reflecting a shift in the protein profile required for maturation. Several proteins, including HIC1, ZMYND11, SORCS3, MEGF6, and DYNLRB1, were upregulated in isthmic secretions as oocytes matured. HIC1, known for its role in genomic stability and cellular homeostasis in cancer biology, may play a similar role in safeguarding oocyte quality during maturation and fertilization (Chen *et al.*, 2005; Van Rechem *et al.*, 2009). While the exact functions of these proteins in oocyte biology remain unclear, their upregulation suggests a regulatory

network that ensures oocyte integrity during maturation and fertilization.

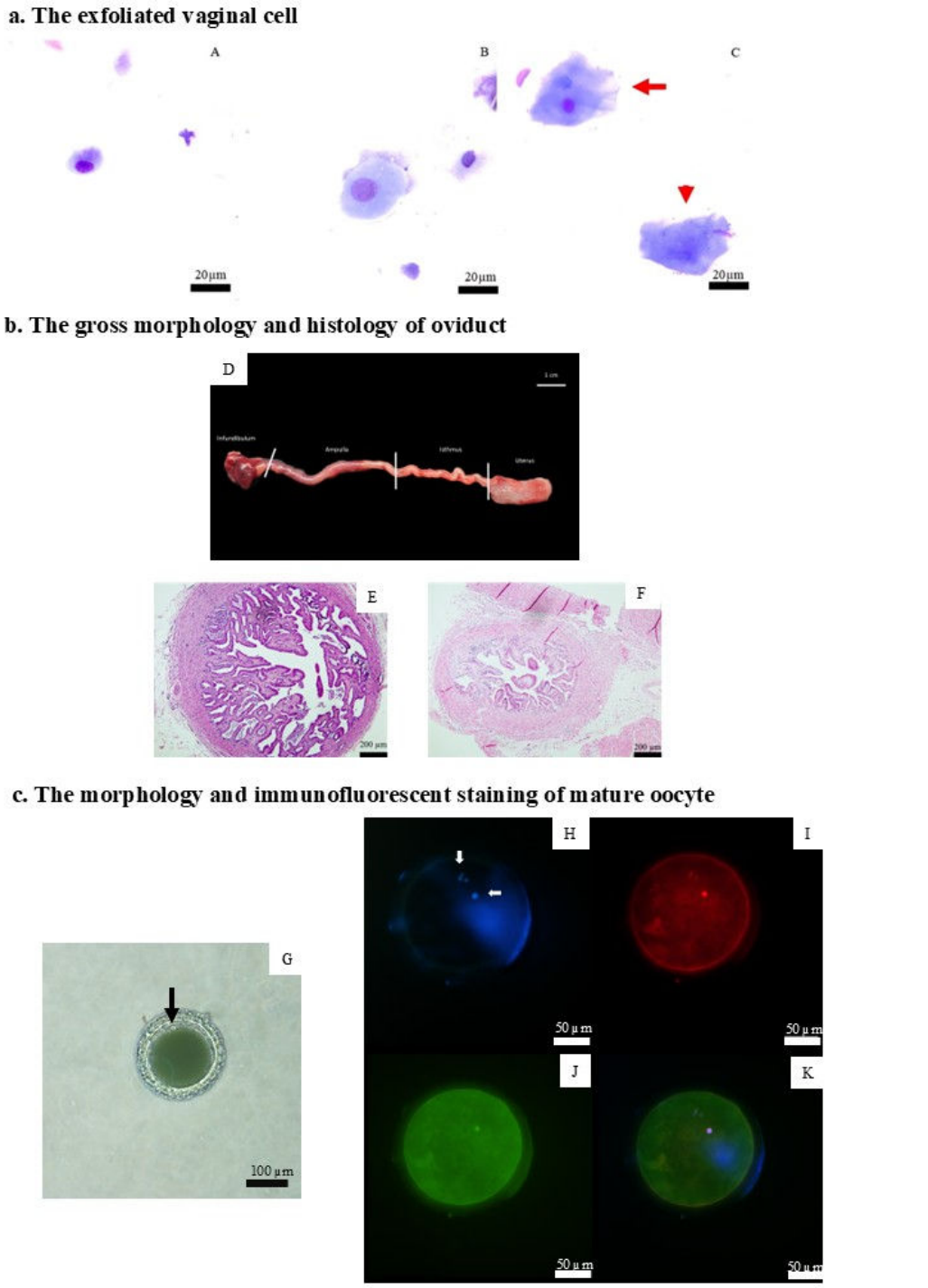

Figure 2 The Exfoliated vaginal canine cell types, gross morphology of oviduct, histopathology of oviduct and oocyte staning. (a) Representative images of exfoliated vaginal cells stained using a cytological stain. Visible cell types include parabasal cells (A), intermediate cells (B), superficial cells (C, arrow), and Anuclear superficial Cell (C, arrowhead), Scale bars = 20 µm. (b) Gross morphology and histological sections of the oviduct stained with hematoxylin and eosin. Gross anatomy showing the infundibulum, ampulla, isthmus, and uterine connection; scale bar = 1 cm (D). The ampulla region shows prominent, highly folded mucosal structures (E), while the isthmus displays a narrower, less convoluted lumen (F), Scale bars = 200 µm. (c) Morphology and staining of mature oocytes. Bright-field image of a mature oocyte displaying the first polar body (black arrow), Scale bar = 100 µm (G). Nuclear staining with DAPI (blue) highlighting the presence of the second metaphase plate, along with the extruded DNA of the first polar body (white arrows) (H). Microtubules were visualized using monoclonal α-tubulin-TRITC staining (I) while microfilaments were labeled with Alexa 488 phalloidin (J). A merged image of all stains is shown in (K). Scale bar = 50 µm.

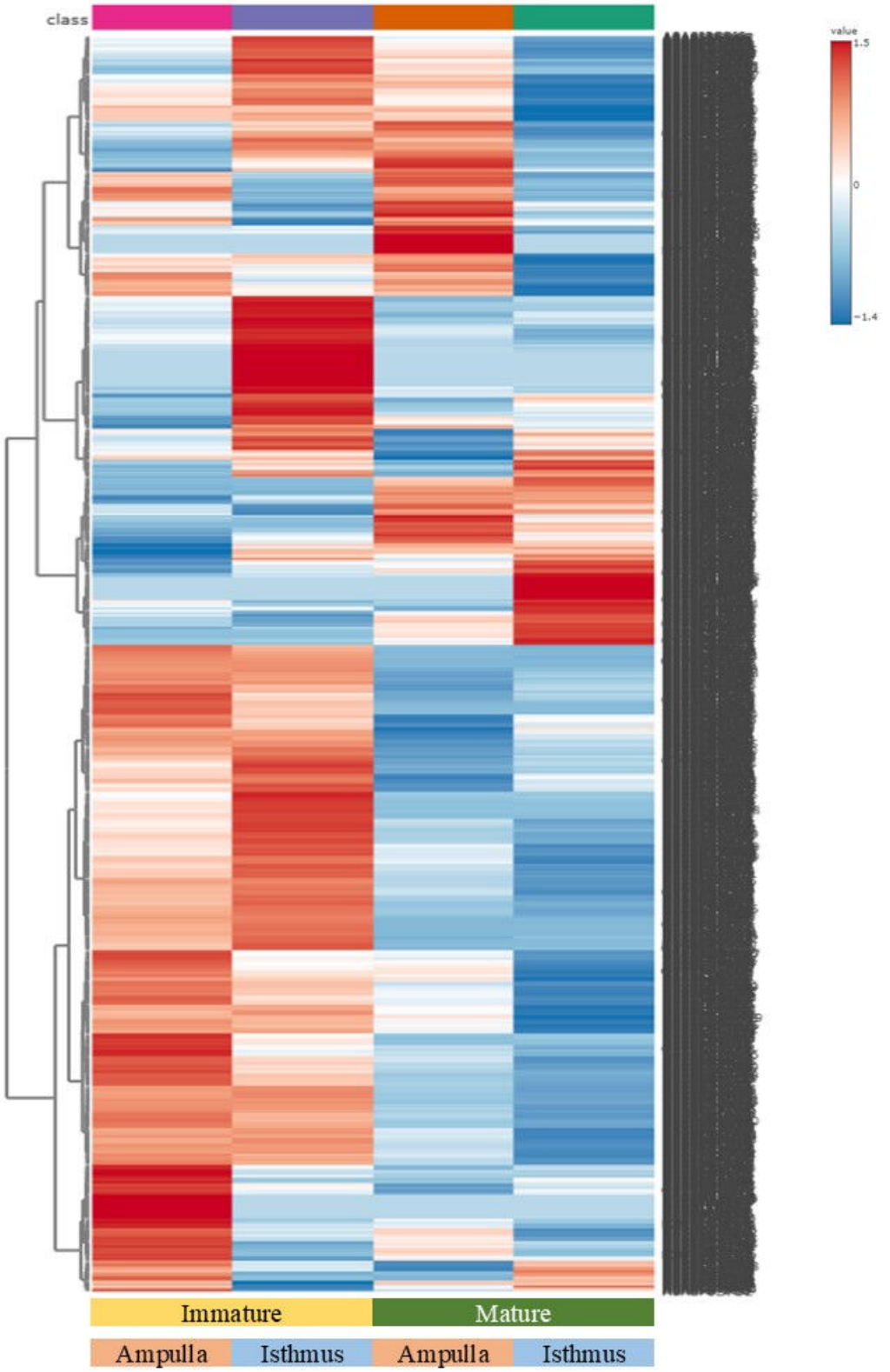

Figure 3 The heat map of identified proteins in canine oviductal secretion. The heatmap illustrates the expression profiles of 16,377 proteins identified in canine oviductal secretions, categorized by oocyte maturity stage (immature vs. mature) and anatomical region (ampulla and isthmus). Each column represents an individual sample, while each row corresponds to a protein with varying expression levels. Protein intensity is color-coded, ranging from very low (deep blue) to extremely high (dark brown). Proteins uniquely upregulated in each group are highlighted in dark red, indicating distinct group-specific expression patterns.

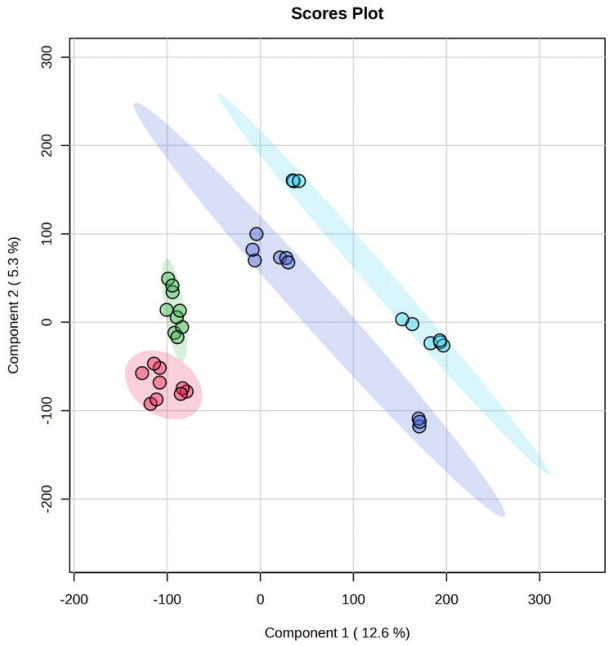

Figure 4 The Partial least squares-discriminant analysis (PLS-DA) scores plot of ampulla secretion samples. Partial least squares-discriminant analysis (PLS-DA) of component one and two in two dimensions was conducted on all identified proteins, with samples clustered according to groups: ampulla fluid with immature oocyte (red), isthmus fluid with immature oocyte (green), ampulla fluid with mature oocyte (dark blue), and isthmus fluid with mature oocyte (light blue). Individual samples are presented by coloured points, with the surrounding coloured regions representing the 95% confidence intervals.

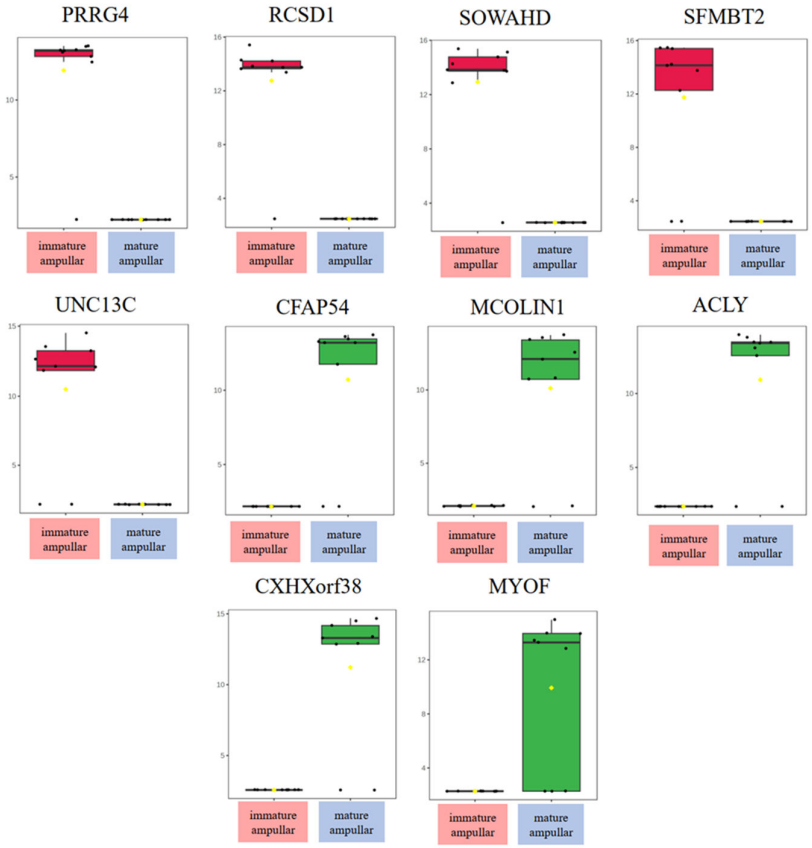

Figure 5 Differential expression of proteins in the ampulla, comparing oocyte maturity stages, including PRRG4, RCSD1, SOWAHD, SFMBT2, UNC13C, CFAP54, MCOLN1, ACLY, CXHXorf38, and MYOF. Ampullary secretions associated with immature oocytes are labeled as 'immature ampullar', while those associated with mature oocytes are labeled as 'mature ampullar'. Proteins highlighted in red were highly expressed during the immature stage, whereas those in green were upregulated during the mature stage.

Figure 6 Protein expression levels in the isthmus were compared between different oocyte maturity stages, including FCHSD1, an uncharacterized protein, LOC119868814, PRKCI, ATP10B, HIC1, ZMYND11, SORCS3, MEGF6, and DYNLRB1. Secretion from the isthmus containing immature oocytes was labeled as 'immature isthmus', while secretion containing mature oocytes was classified as 'mature isthmus'. Proteins shown in the red box exhibited higher expression in the immature oocyte stage, whereas those in the green box were more abundant in the mature oocyte stage.

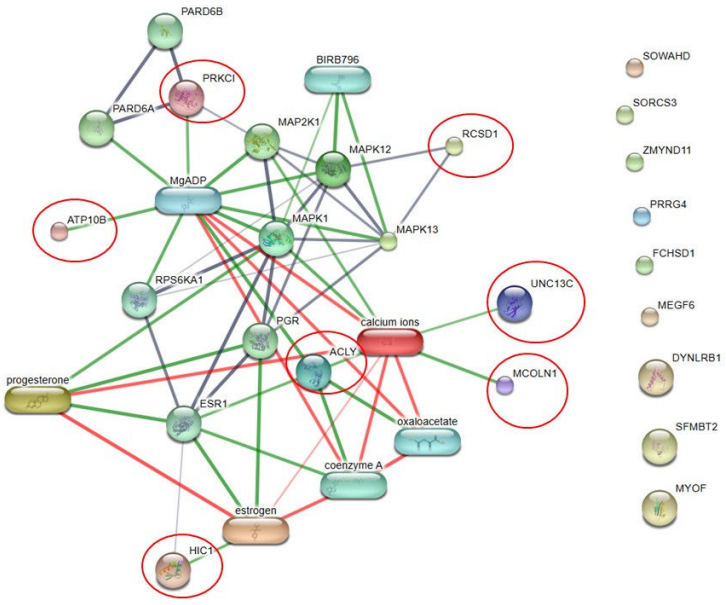

Figure 7 Network of protein–oocyte maturation molecule interactions analyzed by STITCH version 5.0. The diagram illustrates the connections between upregulated and downregulated proteins and their functional partners relevant to oocyte development. The strength of these associations is represented by edge confidence scores: thick lines indicate high-confidence interactions (>0.9), moderate-confidence interactions are shown with medium lines (>0.7), and low-confidence interactions are represented by thin lines (>0.4).

Table 3 The list of top 10 up- and down-regulated proteins in each anatomical region of the oviduct in relation to the stages of oocyte maturation.

Protein ID	Protein name	Gene name	FC	P value	Regulation type
Protein in the ampulla region					
A0A8I3SAE1	Proline rich and Gla domain 4	PRRG4	0.18751	$5.83x10^{-7}$	Down regulation
A0A8C0P6A4	RCSD domain containing 1	RCSD1	0.1941	$6.45x10^{-7}$	Down regulation
A0A8I3PC28	Uncharacterized protein	SOWAHD	0.19912	$7.17x10^{-7}$	Down regulation
A0A8C0LRQ	Scm like with four mbt domains 2	SFMBT2	0.20906	$8.85x10^{-5}$	Down regulation
A0A8C0TUR8	Unc-13 homolog C	UNC13C	0.20925	$8.59x10^{-5}$	Down regulation
A0A8C0QA42	Cilia and flagella associated protein 54	CFAP54	4.8251	$7.85x10^{-5}$	Up regulation
A0A8I3Q7K0	Mucolipin TRP cation channel 1	MCOLN1	4.7657	$9.69x10^{-5}$	Up regulation
A0A8C0P1D8	ATP-citrate synthase	ACLY	4.5516	$7.57x10^{-5}$	Up regulation
A0A8I3Q1F0	Uncharacterized protein	CXHXorf38	4.36	$8.01x10^{-5}$	Up regulation
A0A8C0Z3X7	C2 domain-containing protein	MYOF	4.3497	0.001078	Up regulation
Protein in the isthmus region					
A0A8C0QL61	FCH and double SH3 domains 1	FCHSD1	0.15696	$7.29x10^{-14}$	Down regulation
A0A8I3N5C3	Uncharacterized protein		0.15751	1.90E-20	Down regulation
A0A8I3QCB5	FAM21/CAPZIP domain-containing protein	LOC119868814	0.16263	$3.18x10^{-19}$	Down regulation
A0A8C0PN52	Protein kinase C iota type	PRKCI	0.16542	$1.57x10^{-20}$	Down regulation
A0A8C0N8F8	Phospholipid-transporting ATPase	ATP10B	0.16687	$9.42x10^{-17}$	Down regulation
A0A8P0TIK5	HIC ZBTB transcriptional repressor 1	HIC1	5.3716	0.000102	Up regulation
A0A8C0M7F2	Zinc finger MYND-type containing 11	ZMYND11	5.1906	$9.64x10^{-7}$	Up regulation
A0A8P0SFJ3	Sortilin related VPS10 domain containing receptor 3	SORCS3	4.9938	0.001033	Up regulation
A0A8I3PA47	Multiple EGF like domains 6	MEGF6	4.8209	0.001232	Up regulation
A0A8C0M793	Dynein regulatory complex protein 12	DYNLRB1	4.707	0.000104	Up regulation

In conclusion, this study offers critical insights into the proteomic changes in oviductal secretions in dogs, focusing on protein dynamics during oocyte maturation in the ampulla and isthmus. The findings highlight the complex interplay of proteins involved in essential processes such as cytoskeletal organization, energy metabolism, calcium signaling, and genomic stability, all of which are vital for successful oocyte maturation, fertilization, and early embryonic development.

References

Apparicio M, Alves A, Pires-Butler E, Ribeiro A, Covizzi G and Vicente W 2011. Effects of hormonal supplementation on nuclear maturation and cortical granules distribution of canine oocytes during various reproductive stages. Reproduction in domestic animals. 46: 896-903.

Astudillo I, Aspee K, Palomino J, Peralta OA, Parraguez VH and De los Reyes M 2023. Meiotic Development of Canine Oocytes from Poly-Ovular and Mono-Ovular Follicles after In Vitro Maturation. Animals. 13: 648.

Borges P, Fontaine E, Maenhoudt C, Payan-Carreira R, Santos N, Leblond E, Fontaine C and Fontbonne A 2015. Fertility in adult bitches previously treated with a 4.7 mg subcutaneous deslorelin implant. Reproduction in Domestic Animals. 50: 965-971.

Cao H, Yin X, Cao Y, Jin Y, Wang S, Kong Y, Chen Y, Gao J, Heller S and Xu Z 2013. FCHSD1 and FCHSD2 are expressed in hair cell stereocilia and cuticular plate and regulate actin polymerization in vitro. PLoS One. 8: e56516.

Chen WY, Wang DH, Yen RC, Luo J, Gu W and Baylin SB 2005. Tumor suppressor HIC1 directly regulates SIRT1 to modulate p53-dependent DNA-damage responses. Cell. 123: 437-448.

Concannon PW 2011. Reproductive cycles of the domestic bitch. Animal reproduction science. 124: 200-210.

Croxatto HB 2002. Physiology of gamete and embryo transport through the fallopian tube. Reproductive biomedicine online. 4: 160-169.

Eurell JA and Frappier BL 2013. Dellmann's textbook of veterinary histology. John Wiley & Sons.

Evans HE and De Lahunta A 2012. Miller's Anatomy of the Dog-E-Book: Miller's Anatomy of the Dog-E-Book. Elsevier health sciences.

Fontaine E, Mir F, Vannier F, Gérardin A, Albouy M, Navarro C and Fontbonne A 2011. Induction of fertile oestrus in the bitch using Deslorelin, a GnRH agonist. Theriogenology. 76: 1561-1566.

Gloria A, Contri A, Carluccio A and Robbe D 2018. Blood periovulatory progesterone quantification using different techniques in the dog. Animal reproduction science. 192: 179-184.

He H, Wang J, Mou X, Liu X, Li Q, Zhong M, Luo B, Yu Z, Zhang J and Xu T 2023. Selective autophagic degradation of ACLY (ATP citrate lyase) maintains citrate homeostasis and promotes oocyte maturation. Autophagy. 19: 163-179.

Johnston SD, Kustritz MV and Olson PS 2001. Canine and feline theriogenology.

Kamonpatana M, Kunawongkrit A, Bodhipaksha P and Luvira Y 1979. Effect of PGF-2α on serum progesterone levels in the swamp buffalo (*Bubalus bubalis*). Reproduction. 56: 445-449.

Kumar MA 2015. Clinically oriented anatomy of the dog and cat. Linus Learning.

Kutzler MA, Mohammed HO, Lamb SV and Meyers-Wallen VN 2003. Accuracy of canine parturition date prediction from the initial rise in preovulatory progesterone concentration. Theriogenology. 60: 1187-1196.

Lange-Consiglio A, Perrini C, Albini G, Modina S, Lodde V, Orsini E, Esposti P and Cremonesi F 2017. Oviductal microvesicles and their effect on in vitro maturation of canine oocytes. Reproduction. 154: 167-180.

Lee S, Zhao M, No J, Nam Y, Im GS and Hur TY 2017a. Dog cloning with in vivo matured oocytes obtained using electric chemiluminescence immunoassay-predicted ovulation method. PLoS One. 12: e0173735.

Lee SH, Oh HJ, Kim MJ, Kim GA, Choi YB, Jo YK, Setyawan EMN and Lee BC 2017b. Oocyte maturation-related gene expression in the canine oviduct, cumulus cells, and oocytes and effect of co-culture with oviduct cells on in vitro maturation of oocytes. Journal of Assisted Reproduction and Genetics. 34: 929-938.

Lee SH, Oh HJ, Kim MJ and Lee BC 2020. Canine oviductal exosomes improve oocyte development via EGFR/MAPK signaling pathway. Reproduction. 160: 613-625.

Lee SH and Saadeldin IM 2020. Exosomes as a potential tool for supporting canine oocyte development. Animals. 10: 1971.

Leigh O, Raji L and Diakodue E 2013. Detection of standing heat in bitches: Application of vaginal cytology. World Journal of Life Science and Medical Research. 3: 21-25.

Lopes G, Alves M, Carvalho R, Luvoni G and Rocha A 2011. DNA fragmentation in canine oocytes after in vitro maturation in TCM-199 medium supplemented with different proteins. Theriogenology. 76: 1304-1312.

Lopes G, Sousa M, Luvoni GC and Rocha A 2007. Recovery rate, morphological quality and nuclear maturity of canine cumulus-oocyte complexes collected from anestrous or diestrous bitches of different ages. Theriogenology. 68: 821-825.

Mahrous E, Yang Q and Clarke HJ 2012. Regulation of mitochondrial DNA accumulation during oocyte growth and meiotic maturation in the mouse. Reproduction. 144: 177.

Ntai I, Toby TK, LeDuc RD and Kelleher NL 2016. A method for label-free, differential top-down proteomics. Quantitative Proteomics by Mass Spectrometry. 1410: 121-133.

Ponglowhapan S, Suthamnatpong A, Khamanarong A, Akaraphutoporn E, Jamikorn U and Kulabsri S 2018. Failure to conceive in deslorelin-induced oestrous bitches with regard to removal of hormone implants after ovulation. The Thai Journal of Veterinary Medicine. 48: 211-217.

Reckers F, Klopfleisch R, Belik V and Arlt S 2022. Canine vaginal cytology: a revised definition of exfoliated vaginal cells. Frontiers in Veterinary Science. 9: 834031.

Reynaud K, Fontbonne A, Marseloo N, de Lesegno CV, Saint-Dizier M and Chastant-Maillard S 2006. In vivo canine oocyte maturation, fertilization and early embryogenesis: A review. Theriogenology. 66: 1685-1693.

Saint-Dizier M, Marnier C, Tahir MZ, Grimard B, Thoumire S, Chastant-Maillard S and Reynaud K 2014. OVGP1 is expressed in the canine oviduct at the time and place of oocyte maturation and fertilization. Molecular Reproduction and Development. 81: 972-982.

Simerly C and Schatten G 1993. Techniques for localization of specific molecules in oocytes and embryos, In: Methods in enzymology. Elsevier. pp. 516-553.

Songsasen N, Yu I and Leibo S 2002. Nuclear maturation of canine oocytes cultured in protein-free media. Molecular Reproduction and Development: Incorporating Gamete Research. 62: 407-415.

Sturmey R, Reis A, Leese H and McEvoy T 2009. Role of fatty acids in energy provision during oocyte maturation and early embryo development. Reproduction in Domestic Animals. 44: 50-58.

Su YQ and Eppig JJ 2002. Evidence that multifunctional calcium/calmodulin-dependent protein kinase II (CaM KII) participates in the meiotic maturation of mouse oocytes. Molecular reproduction and development. 61: 560-569.

Tsutsui T and Shimizu T 1975. Studies on the reproduction in the dog IV. On the fertile period of ovum after ovulation. The Japanese journal of animal reproduction. 21: 65-69.

Tyanova S, Temu T and Cox J 2016. The MaxQuant computational platform for mass spectrometry-based shotgun proteomics. Nature protocols. 11: 2301-2319.

Van Rechem C, Rood BR, Touka M, Pinte S, Jenal M, Guérardel C, Ramsey K, Monté D, Bégue A and Tschan MP 2009. Scavenger chemokine (CXC motif) receptor 7 (CXCR7) is a direct target gene of HIC1 (hypermethylated in cancer 1). Journal of biological chemistry. 284: 20927-20935.

Vannucchi CI, de Oliveira CM, Marques MG, Assumpçao MEOA and Visintin JA 2006. In vitro canine oocyte nuclear maturation in homologous oviductal cell co-culture with hormone-supplemented media. Theriogenology. 66: 1677-1681.

Wakai T, Vanderheyden V, Yoon SY, Cheon B, Zhang N, Parys JB, Fissore RA 2012. Regulation of inositol 1, 4, 5-trisphosphate receptor function during mouse oocyte maturation. Journal of cellular physiology. 227: 705-717.

Walter B, Otzdorff C, Brugger N and Braun J 2011. Estrus induction in Beagle bitches with the GnRH-agonist implant containing 4.7 mg Deslorelin. Theriogenology. 75: 1125-1129.

Wang Y, Wang J, Chen L, Chen Z, Wang T, Xiong S, Zhou T, Wu G, He L and Cao J 2023. PRRG4 regulates mitochondrial function and promotes migratory behaviors of breast cancer cells through the Src-STAT3-POLG axis. Cancer cell international. 23: 323.

Xiao H and Liu M 2013. Atypical protein kinase C in cell motility. Cellular and molecular life sciences. 70: 3057-3066.